AD-A141 813 SCHOTTKY BARRIER PHOTOELECTRODES WITH A VARIABLE BARRIER HEIGHT(U) EIC LABS INC NORWOOD MA R D RAUH ET AL. MAY 84 C-757 N00014-83-C-0763 1/1

UNCLASSIFIED F/G 20/12 NL

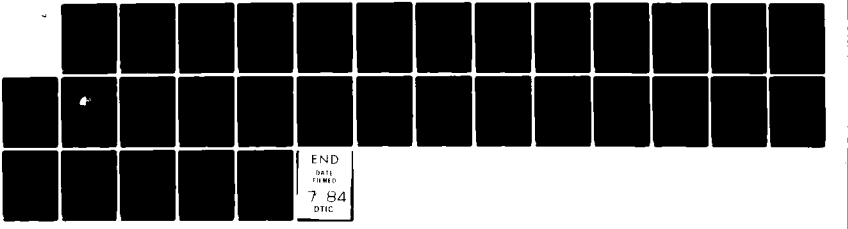

END
DATE FILMED
7 84
DTIC

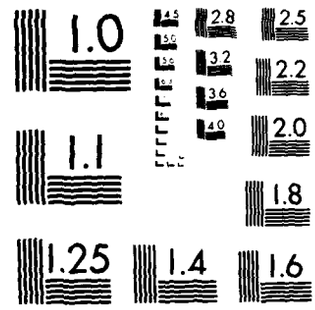

Report N00014-83-C-0763

SCHOTTKY BARRIER PHOTOELECTRODES WITH A VARIABLE BARRIER HEIGHT

R. David Rauh and Douglas R. Rogers

EIC Laboratories, Inc.
111 Downey Street
Norwood, Massachusetts 02062

May, 1984

Final Report for Period 26 September 1983 - 25 March 1984
Approved for Public Release - Distribution Unlimited

Prepared for

OFFICE OF NAVAL RESEARCH
Department of the Navy
800 North Quincy Street
Arlington, Virginia 22217

Disclaimers

The views and conclusions contained in this document are those of the authors and should not be interpreted as necessarily representing the official policies, either expressed or implied, of the Office of Naval Research or the U.S. Government.

The citation of trade names and names of manufacturers in this report is not to be construed as official government endorsement or approval of commercial products or services referenced herein.

UNCLASSIFIED

SECURITY CLASSIFICATION OF THIS PAGE (When Data Entered)

REPORT DOCUMENTATION PAGE	READ INSTRUCTIONS BEFORE COMPLETING FORM
1. REPORT NUMBER N00014-83-C-0763 AD-A141813	3. RECIPIENT'S CATALOG NUMBER
4. TITLE (and Subtitle) SCHOTTKY BARRIER PHOTOELECTRODES WITH A VARIABLE BARRIER HEIGHT	5. TYPE OF REPORT & PERIOD COVERED FINAL REPORT 26 Sep 83-25 Mar 84
	6. PERFORMING ORG. REPORT NUMBER C-757
7. AUTHOR(s) R. David Rauh and Douglas R. Rogers	8. CONTRACT OR GRANT NUMBER(s) N00014-83-C-0763
9. PERFORMING ORGANIZATION NAME AND ADDRESS EIC Laboratories, Inc. 111 Downey Street Newton, MA Norwood, Massachusetts 02158	10. PROGRAM ELEMENT PROJECT, TASK AREA & WORK UNIT NUMBERS NR SBI-002
11. CONTROLLING OFFICE NAME AND ADDRESS Office of Naval Research 800 North Quincy Street Arlington, VA 22217	12. REPORT DATE MAY 1984 13. NUMBER OF PAGES 29
14. MONITORING AGENCY NAME & ADDRESS(if different from Controlling Office)	15. SECURITY CLASS. (of this report) UNCLASSIFIED 15a. DECLASSIFICATION/DOWNGRADING SCHEDULE

16. DISTRIBUTION STATEMENT (of this Report)

Approved for public release; distribution unlimited.

17. DISTRIBUTION STATEMENT (of the abstract entered in Block 20, if different from Report)

18. SUPPLEMENTARY NOTES

19. KEY WORDS (Continue on reverse side if necessary and identify by block number)

Photoelectrochemistry, Schottky Barrier, Diode, Barrier Height, Silicon, Ion Insertion, Tungsten Trioxide, Intercalation, Sensors

20. ABSTRACT (Continue on reverse side if necessary and identify by block number)

The purpose of this research is to investigate the properties of Schottky barriers formed between semiconductors and ion insertion compounds having continuously and reversibly variable work functions. In Phase I, the diode p-Si/M_xWO_3 (M = H, Li) was studied. Li_xWO_3 thin films, prepared by vacuum evaporation or sputtering, showed work functions spanning the range 4.2-5.2 eV for x = 0 to 0.4. Electrical measurements on solid state diodes

DD FORM 1 JAN 73 1473 EDITION OF 1 NOV 65 IS OBSOLETE

UNCLASSIFIED

SECURITY CLASSIFICATION OF THIS PAGE (When Data Entered)

20. Abstract (Cont.)

employing Li_xWO_3 layers revealed a barrier height modulation of 0.06V for this range, limited by significant Fermi level pinning. Photoelectrochemical measurements of H_xWO_3 coated p-Si electrodes showed that the ion insertion compound enhanced electrode stability and photoresponse in acidic electrolytes. The band bending in naked and coated p-Si electrodes was measured as a function of applied bias using a new technique assessing saturation photovoltage as the electrode is polarized. The slope of these curves, (dV_B/dV), is related inversely to the interface state density, D_S. D_S was significantly reduced by the H_xWO_3 overlayer.

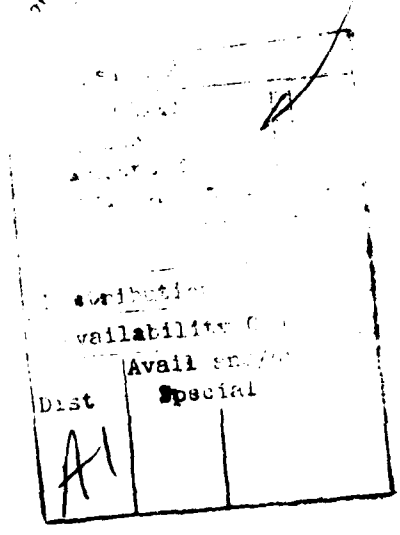

U.S. DEPARTMENT OF DEFENSE

SMALL BUSINESS INNOVATION RESEARCH PROGRAM
PHASE I—FY 1983
PROJECT SUMMARY

FOR DOD USE ONLY

Program Office	Proposal No.	Topic No.

TO BE COMPLETED BY PROPOSER

Name and Address of Proposer

EIC Laboratories, Inc.
111 Downey Street
Norwood, MA 02062

Name and Title of Principal Investigator

R. David Rauh, Director of Research

Title of Project

Schottky Barrier Photoelectrodes with a Variable Barrier Height

Technical Abstract (Limit to two hundred words)

The purpose of this research is to investigate the properties of Schottky barriers formed between semiconductors and ion insertion compounds having continuously and reversibly variable work functions. In Phase I, the diode p-Si/M_xWO_3 (M = H, Li) was studied. Li_xWO_3 thin films, prepared by vacuum evaporation or sputtering, showed work functions spanning the range 4.2-5.2 eV for x = 0 to 0.4. Electrical measurements on solid state diodes employing Li_xWO_3 layers revealed a barrier height modulation of 0.06V for this range, limited by significant Fermi level pinning. Photoelectrochemical measurements of H_xWO_3 coated p-Si electrodes showed that the ion insertion compound enhanced electrode stability and photoresponse in acidic electrolytes. The band bending in naked and coated p-Si electrodes was measured as a function of applied bias using a new technique assessing saturation photovoltage as the electrode is polarized. The slope of these curves, (dV_B/dV), is related inversely to the interface state density, D_S. D_S was significantly reduced by the H_xWO_3 overlayer.

Anticipated Benefits/Potential Commercial Applications of the Research or Development

Variable barrier height diodes have numerous Naval and commercial applications. Insertion compounds provide chemically sensitive layers so that such diodes would find applications as sensors for intercalating species, e.g., hydrogen, ammonia and other strong electron donors/acceptors. In addition, junctions between semiconductors and electrochromic ion insertion layers have uses as electro-optical imagers and image enhancers. Other uses include fuel-forming photoelectrodes with improved stability and efficiency.

TABLE OF CONTENTS

		Page
	PROJECT SUMMARY.	iii
1.0	INTRODUCTION	1
2.0	PHASE I RESEARCH: EXPERIMENTAL.	5
	2.1 Materials and Schottky Barrier Fabrication.	5
	2.2 Electrical Measurements	6
	2.3 Electrochemical Measurements.	6
3.0	PHASE I RESEARCH: RESULTS	8
	3.1 Li_xWO_3 Reversible Potential	8
	3.2 Capacitance-Voltage Behavior.	8
	3.3 Current-Voltage Behavior.	13
	3.4 $Al\|p\text{-}Si\|WO_3$ Photoelectrochemical Response	15
4.0	SUMMARY AND CONCLUSIONS.	22
5.0	REFERENCES	24

LIST OF FIGURES

		Page
Fig. 1	Principle of variable Schottky barrier height using an ion insertion metal contact (C_xAB_n)	2
Fig. 2	Test structure for Ni|Li_xWO_3(0.5μ)|p-Si|Al ohmic contact Schottky barriers	7
Fig. 3	Equilibrium potentials of WO_3 with varying amounts of Li, measured electrochemically in propylene carbonate vs. V(Li^+/Li)	9
Fig. 4	Capacitance-voltage and Mott-Schottky ($1/C^2$ vs. V) plots of p-Si diodes	11
Fig. 5	C-V and $1/C^2$ vs. V plots of p-Si|Li_xWO_3|Ni diodes. . .	12
Fig. 6	Representative forward current characteristics for p-Si|Li_xWO_3|Ni Schottky barrier diodes	14
Fig. 7	Variation of barrier height with metal work function (ϕ_m) in Ni|Li_xWO_3|p-Si diodes.	16
Fig. 8	Current-voltage curves for p-Si and p-Si|0.5 μ WO_3 photocathodes under ∿1 mW/cm^2 633 nm illumination. . .	17
Fig. 9	Photovoltage vs. voltage for p-Si photoelectrodes with and without 0.5 μm WO_3.	19
Fig. 10	Development of Schottky barrier during photoelectrochemical reduction of WO_3 overlayer on a p-type semiconductor.	20
Fig. 11	Index of interface behavior vs. metal-semiconductor electronegativity difference for various semiconductors.	23

1.0 INTRODUCTION

Most solid state electronic semiconductor devices are dependent on the properties of the rectifying junction which forms between the semiconductor and a contacting phase of differing work function. In this program, we consider a novel device structure in which the interface energetics can be, in principle, controlled in a continuous and reversible manner.

To date, Schottky barriers have been produced using elemental metal or metal alloy (e.g., PtSi) contacts (1). In order to provide a variable contact potential and to sample effective work functions outside of the regions normally found in these metals, thin film insertion compounds may be employed as barrier metals. The ion insertion reaction can be generalized as

$$AB_n + xC^{m+} + mxe^- \rightleftarrows C_xAB_n \qquad [1]$$

The same reaction may be promoted chemically, e.g., by reaction of solid AB_n with C in the gas phase:

$$AB_n + xC \rightleftarrows C_xAB_n \qquad [2]$$

An example of this reaction is the reversible insertion of H, Li or Na into the perovskite WO_3. When carried out electrochemically, the reaction potentials for WO_3 thin films appear to be smoothly varying functions of composition. For $0<x<1$, the potential varies by at least 1V. If the compound C_xAB_n is in direct contact with a semiconductor surface, then the effective Schottky barrier height should be directly proportional to the chemical potential of the reversible reaction (1). The variable barrier height concept is illustrated in Figure 1 for a Schottky barrier where the work function change in C_xAB_n is promoted electrochemically.

Numerous ion insertion compounds with approximately reversible electrochemical behavior have been identified as a result of technological interest in electrochromism (2) and high energy density Li or Na batteries (3). A representative group of these materials and their relevant properties are given in Table 1. These nonstoichiometric compounds span a range of potentials (and hence electron energies) from -2V to +2V vs. the standard hydrogen potential. On an electron energy scale, this range corresponds to $\sim$2.5 to 6.5 eV. Insertion compounds containing 2 or even 3 elements can be fabricated as thin films by evaporation or sputtering processes. We note that only a few monolayers of metal are required to form a Schottky barrier. Hence, variable barrier height photoelectric or photoelectrochemical devices can be conceived, where light absorption from the insertion compound is minimal.

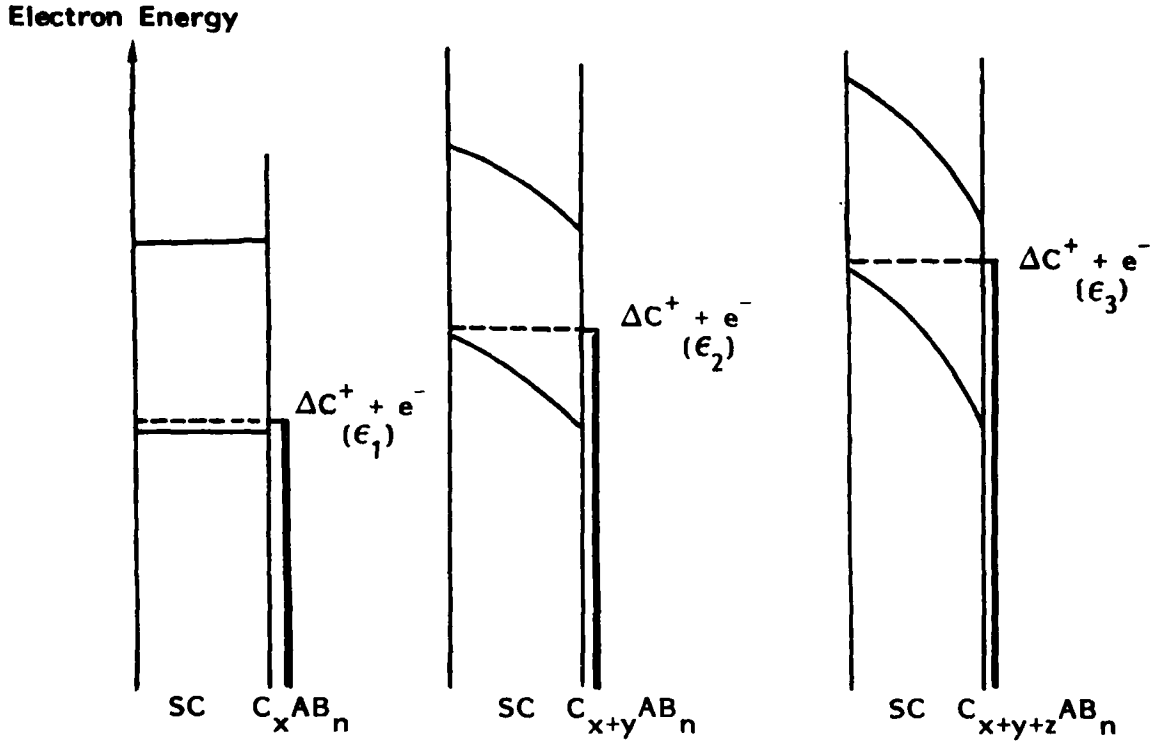

Fig. 1. Principle of variable Schottky barrier height using an ion insertion metal contact (C_xAB_n). The potential of the reaction

$$\Delta C^+ + C_{x-\Delta}AB_n + \Delta e^- \rightleftarrows C_xAB_n$$

becomes increasingly negative as x is increased, due to a simultaneous increase in the energy of electrons in the nonstoichiometric compound. Note that only a few monolayers of C_xAB_n are necessary to establish the interface potential.

TABLE 1

SOME ALKALI AND HYDROGEN ION INSERTION REACTIONS
AND ASSOCIATED POTENTIAL RANGES

Ion Insertion Reaction	Potential Range vs. M^+/M[1]	Absolute Electron Energy Range[2] (eV)
$WO_2/LiWO_3$	1.1/0.3	3.0/2.2
$WO_3/LiWO_3$	3.0/1.5	4.9/3.4
$WO_3/NaWO_3$	3.0/1.6	4.9/3.6
WO_3/HWO_3	0.4/-0.5[3]	4.9/4.1
TiS_2/Li_2TiS_2	2.4/0.5	4.3/2.4
$CuS/Li_{1.2}CuS$	2.0/1.3	3.9/3.2
$RuO_2/LiRuO_2$	1.2/0.4	3.1/2.3
$RuO_2/HRuO_2$	1.5/0	6.1/4.6
V_6O_{13}/LiV_6O_{13}	2.9/1.3	4.8/3.2
$CrO_{2.5}/LiCrO_{2.5}$	3.9/1.1	5.8/3.0
$MoO_3/LiMoO_3$	2.5/1.3	4.4/3.2
$CoO_2/LiCoO_2$	4.7/3.9	6.6/5.8
$(CH)_x/Li(CH)_x$	4.0/$\sim$1.0	5.9/2.9
$IrO_2 \cdot H_2O/Ir(OH)_3$	0.3/-0.8	4.9/3.8

[1] V vs. (Li^+/Li) measured in propylene carbonate. $V(H^+/H_2)$ is the normal hydrogen electrode (NHE). $NHE_{aq} \approx 2.71V$ vs. $V(Li^+/Li)$ in propylene carbonate (N. Matsuura, K. Umimoto and Z. Takeuchi, Bull. Chem. Soc. Japan 47, 813 (1974)).

[2] Assuming NHE = 4.6 eV below vacuum; $E°(Li^+/Li)$ in propylene carbonate = 1.9 eV below vacuum.

[3] Unstable in aqueous solution.

The compounds in Table 1 all have work functions which are variable with H, Li or Na content. These elements may be introduced by either reactions [1] or [2]. We note further that the variable barrier height Schottky diodes are chemical sensors for these elements. The same principles may be applied to insertion compounds of the general formula C_xAB_n, i.e., where AB_n = a layered compound such as TaS_2 and C is an organic base/electron donor (e.g., pyridine)(4). Thus, although not addressed in Phase I, this concept might be applied to a wide range of chemical sensors. Again, the fact that the barrier need only be a few monolayers thick would contribute to the enhanced sensitivity of such devices.

In the Phase I research, we were able to conduct preliminary experiments on solid state and photoelectrochemical characterization of one model system, the p-Si/M_xWO_3 Schottky barrier. Here we were able to demonstrate the feasibility of constructing such an element with M = Li and x variable. The results of the six-month research effort are given in Sections 2.0 and 3.0; the summary and conclusions in Section 4.0.

2.0 PHASE I RESEARCH: EXPERIMENTAL

2.1 Materials and Schottky Barrier Fabrication

Schottky barriers were fabricated onto <111> p-Si wafers obtained from Virginia Semiconductors, Inc., Fredericksburg, VA 22401. The wafers were p-type, B doped, with resistivities of 2 to 16 Ω-cm. This corresponds to a range of doping densities of 7×10^{15} to 8×10^{14} cm^{-3}.

Alloyed Al-Si ohmic contacts were formed on the unpolished face of the wafer. The evaporations were carried out thermally using an Edwards 3-source system. The Al was evaporated from a tungsten filament at 10^{-6} torr and a Si substrate temperature which increased from 62 to 240°C during the process. After deposition of the Al, the substrate was heated radiatively from the tungsten filament to 500°C, *in vacuo*, for 3 minutes. This procedure resulted in an Al-Si alloy ohmic contact, which was verified by the symmetrical i-V characteristics of two separated dots.

Ni was used for top contacts, since it is mechanically robust and not easily scratched during probe measurements. The polished surface of the p-Si was prepared by degreasing with spectroscopic grade methanol, acetone, and methyl ethyl ketone. The surface was then etched for 15 seconds in concentrated HF, rinsed with triply distilled H_2O, and immediately introduced into the vacuum chamber. About 500Å of Ni was evaporated at 4×10^{-6} torr from an alumina coated tungsten boat through a mask containing regions 0.045 cm^2 and 0.0015 cm^2 circles in contact with the Si wafer.

Diodes of configuration Ni|WO_3|p-Si|Al were produced by evaporating ∿5000Å of WO_3 onto the p-Si polished surface following the above cleaning/etching procedure. An alumina coated tungsten boat and a pressure of $2\text{-}4 \times 10^{-5}$ torr were employed. A Kronos quartz crystal thickness monitor was employed for *in situ* monitoring of the process. However, all film thicknesses were measured following evaporation with a Sloan Dektak profilimeter. These two measurements of film thickness generally agreed to within 10%.

Li metal was evaporated onto the WO_3 film using the thickness monitor to measure the amount and hence the Li_xWO_3 stoichiometry. The density of WO_3 films formed under these conditions is ∿6g/cm^3. Thus, the stoichiometry x = 1 is achieved with a Li:WO_3 thickness ratio of 1/3. During the Li evaporation, a shutter was moved across the WO_3 film, and controlled amounts of Li were deposited onto 4 regions, representing x = 0.1, 0.2, 0.3 and 0.4. Following Li evaporation, the substrate

temperature was raised to 350°C for 3 minutes, to promote the completion of Li_xWO_3 formation. A glass slide also coated with WO_3 was placed beside the Si wafer during this process and was also coated with Li. The rapid blue coloration of the Li_xWO_3 could, therefore, be monitored visually. The reaction appeared to be immediate, with no further change in color appearing during the annealing step. The four Li_xWO_3 regions could be seen easily on the glass slide, with mask-defined boundaries separating regions of deepening blue coloration. Finally, without breaking vacuum, the diode hole mask and Ni evaporation source were moved into place, and circular Ni top contacts evaporated over the Li_xWO_3. A typical test wafer is shown in Figure 2. Each region contained from 5 to 25, 0.045 cm^2 diodes for test.

2.2 Electrical Measurements

The capacitance-voltage (C-V) and current voltage (j-V) characteristics of the diodes were measured using standard apparatus. The wafers were mounted on a Signatone temperature controlled vacuum chuck, and the diodes were contacted with a small Ni wire loop probe. Capacitance was measured at 1 MHz with a Boonton 72BD capacitance meter. The device bias was produced using a voltage ramp output from a Princeton Applied Research Model 173 Universal programmer. The resulting C-V curve was plotted on a Hewlett Packard 7013B x-y recorder. Current-voltage curves were obtained using a PAR Model 373 potentiostat, driven with the same voltage ramp. The apparatus was configured so that the C-V and j-V curve could be obtained sequentially on the same diode without moving the device or the probe.

2.3 Electrochemical Measurements

Measurements of Li_xWO_3 potentials were carried out in propylene carbonate, 1N $LiClO_4$, vs. a Li^+/Li reference electrode. These experiments were conducted in an Ar atmosphere glove box containing <10 ppm H_2O. Equilibrium potentials were obtained with a Keithly electrometer.

Photoelectrochemical measurements were carried out in a demountable Teflon cell. The cell permits rapid mounting of ~0.5 cm^2 pieces cut from the p-Si wafers. A key component of the cell is the conductive rubber contact (Chromerics Materials, Inc., Woburn, MA), which forms a compliant contact to the ohmic side of the fragile wafer (5). These measurements were made in an aqueous 0.1M HCl electrolyte. An Ag/AgCl wire reference electrode was employed which had a measured equilibrium potential of +0.058V vs. SCE. Some measurements were made using a Metrologic 3 mW He-Ne laser operating at 633 nm. Measurements of photovoltage vs. applied voltage were made using pulsed dye laser excitation. This apparatus has been described elsewhere (6).

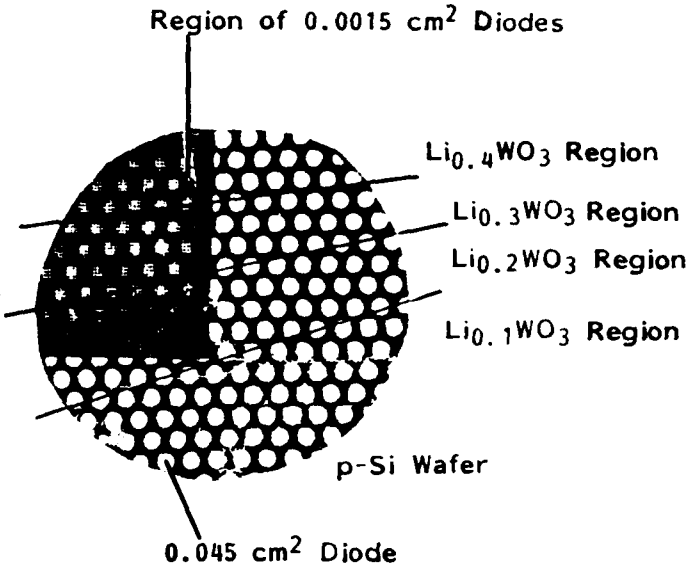

Fig. 2. Test structure for Ni|Li_xWO_3(0.5μ)|p-Si|Al ohmic contact Schottky barriers. Li is introduced by evaporation into selectively masked areas. Circles are Ni contacts, 0.045 cm^2 and 0.0015 cm^2.

Structures evaluated: Ni|p-Si|Al

Ni|WO_3(0.5μ)|p-Si|Al

Ni|Li_xWO_3(0.5μ)|p-Si|Al

3.0 PHASE I RESEARCH: RESULTS

3.1 Li_xWO_3 Reversible Potential

The evaporated WO_3 films were featureless by X-ray and were thus judged to be amorphous. Nevertheless, we determined the variation of Li_xWO_3 potential as a function of x for amorphous films prepared by rf sputtering as well as by evaporation, and also for crystalline films prepared by rf sputtering onto a substrate heated to 350°C. WO_3 films, 0.5μ thick, were deposited onto conductive SnO_{2-x} coated glass (PPG Industries). The reaction $xLi^+ + xe^- + WO_3 \rightarrow Li_xWO_3$ was carried out galvanostatically. In general, 25 minutes were allowed between each Li insertion to permit the electrochemical cell to equilibrate. The results are shown in Figure 3.

The equilibrium potential for both the amorphous and crystalline films changes rapidly on Li insertion. These results are similar to those obtained by other investigators (7,8). During the measurement of the potential it was found that the observed EMF frequently took an extensive length of time to reach its true equilibrium value. The locations of the interrupts and the time lengths are shown in Figure 3. The fact that it takes such a long time to reach equilibrium indicates that bulk diffusion in the Li_xWO_3 films is governing the kinetic behavior. The inserted Li initially accumulates at the film-electrolyte interface and then diffuses slowly through the bulk of the WO_3 until the Li concentration is uniform.

Measurements of the potentials of Li_xWO_3 formed by evaporation of Li rather than by electrochemical incorporation fell into the range corresponding to their stoichiometry as measured by the *in situ* thickness monitor, using the amorphous Li_xWO_3 curve in Figure 3.

An energy scale is also provided in Figure 3 which relates the equilibrium Li_xWO_3 potential to the vacuum scale. This scale is derived from the fact that the standard H_2 potential is determined experimentally to be ~4.6 eV vs. vacuum, and that $E°(Li^+/Li) = -2.7V$ vs. NHE_{aq} (9,10). Hence, a work function range of 4.1 to 5.3 eV is obtained for a-Li_xWO_3, with x varied from 0 to 0.4. This large variation may be obtained either by electrochemical reduction of Li^+ onto WO_3, or by reaction of Li metal with WO_3, with similar results.

3.2 Capacitance-Voltage Behavior

C-V measurements were obtained at 1 MHz for the entire series of $Ni|Li_xWO_3|p\text{-}Si|Al$ diodes (x = 0, 0.1, 0.2, 0.3, 0.4). At least 5 diodes

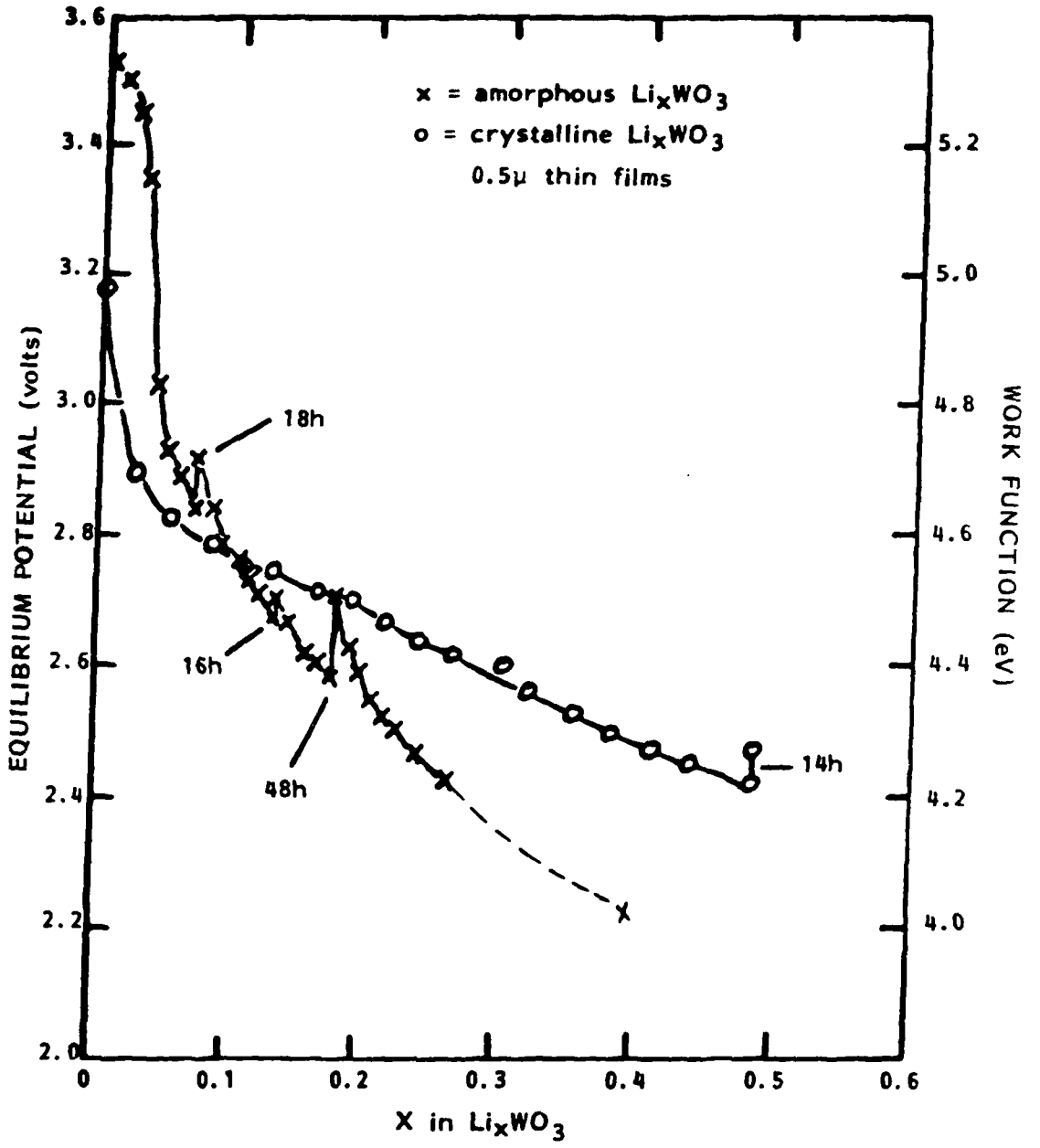

Fig. 3. Equilibrium potentials of WO_3 with varying amounts of Li, measured electrochemically in propylene carbonate vs. $V(Li^+/Li)$.

were evaluated in each region of stoichiometry. All diodes showed rectifying behavior. Representative plots for the diodes under test are shown in Figures 4 and 5. Measurements in the different regions were virtually superimposable except for the x = 0.1 region, which showed about 20% variance in capacitance from structure to structure. Since x = 0.1 is in the steep region of potential variation (Figure 3), this may be a result of small variations in stoichiometry. In general, capacitance values were an inverse function of Li content in the films. This suggests the increased barrier heights accompany decreased work function of the Li_xWO_3 layer.

The C-V behavior of metal-semiconductor contacts may be understood in terms of modulation of the space charge, Q_{sc}, with applied voltage. Using the notation in Sze (1), the junction capacitance is given as

$$C \equiv \left|\frac{\partial Q_{sc}}{2V}\right| = \left[\frac{q\varepsilon_s N_A}{2(V_{bi}-V-kT/q)}\right]^{\frac{1}{2}} \qquad [3]$$

Here, N_A is the doping density, ε_s is the semiconductor permittivity (1.05×10^{-12} F/cm for Si), and V_{bi} is the built-in potential. A straight line is obtained if $1/C^2$ is plotted vs. V, since

$$\frac{1}{C^2} = \frac{2(V_{bi}-V-kT/q)}{q\varepsilon_s N_A} \qquad [4]$$

The doping density is given by the slope:

$$N_A = \frac{2}{q\varepsilon_s}\left[\frac{1}{d(1/C^2)/dV}\right] \qquad [5]$$

The intercept, V_i, is approximately related to the barrier height, ϕ_{B_p}, by the expression

$$\phi_{B_p} = V_i + V_p + kT/q \qquad [6]$$

At 10^{15} cm^{-3} doping concentration, V_p = 0.25V, i.e., the Fermi level is 0.25 eV above the valence band.

In Figures 4 and 5, plots of $1/C^2$ vs. V are shown for the same diodes. All are classically linear and show slopes which yield acceptor densities of 3×10^{15} to 3×10^{16} cm^{-3}, which is in the range of the wafers employed (7×10^{15} cm^{-3}). However, N_A values for lithiated diodes are slightly lower, suggesting some possible compensation of acceptors by Li during fabrication. The x intercepts of the $1/C^2$ vs. V plots yield barrier heights of 0.7-0.8V, somewhat higher than expected for Ni|p-Si diodes. Table 2 summarizes results of barrier heights and doping densities obtained from C-V measurements.

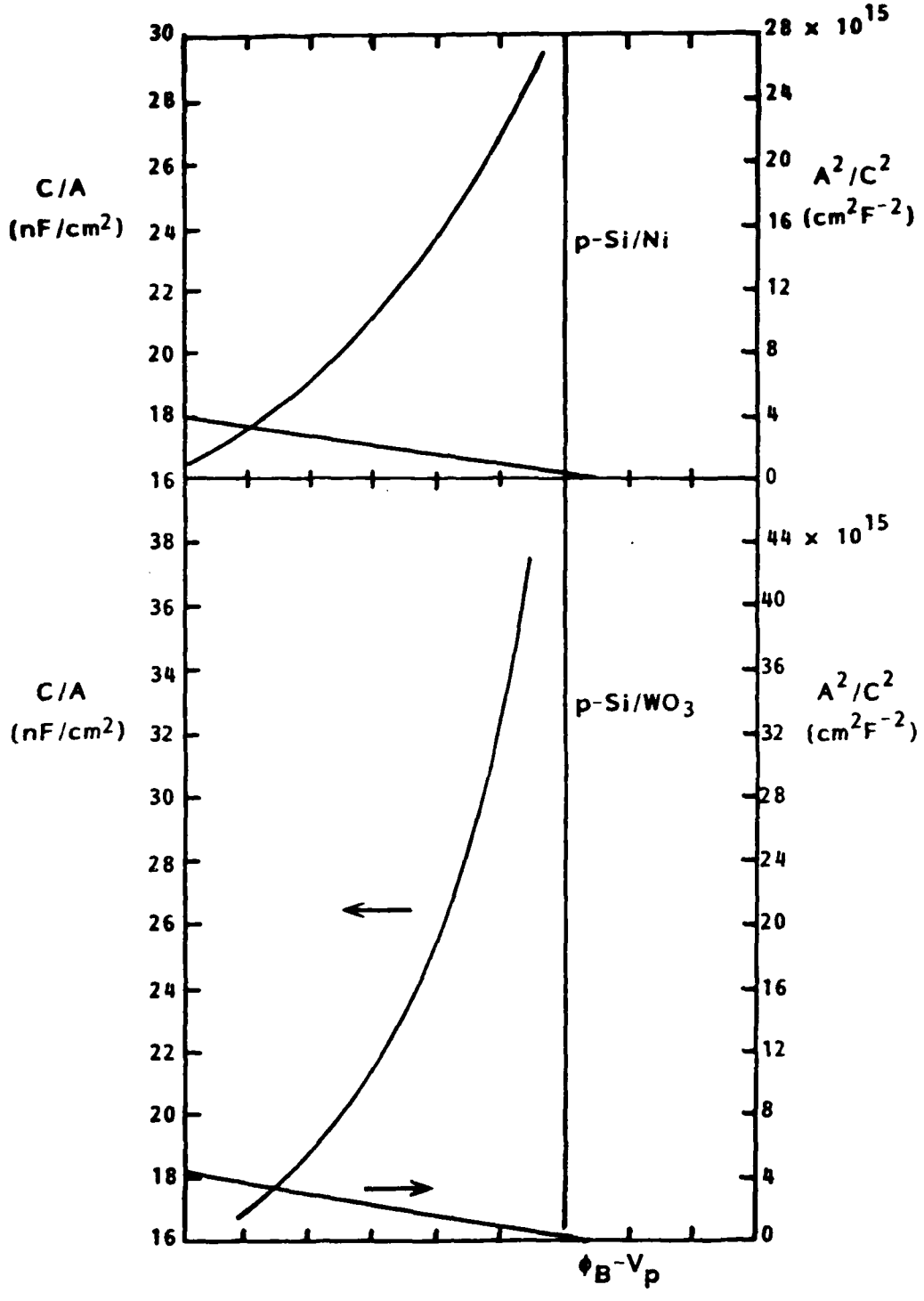

Fig. 4. Capacitance-voltage and Mott-Schottky ($1/C^2$ vs. V) plots of p-Si diodes. Frequency = 1 MHz, ±15 mV rms.

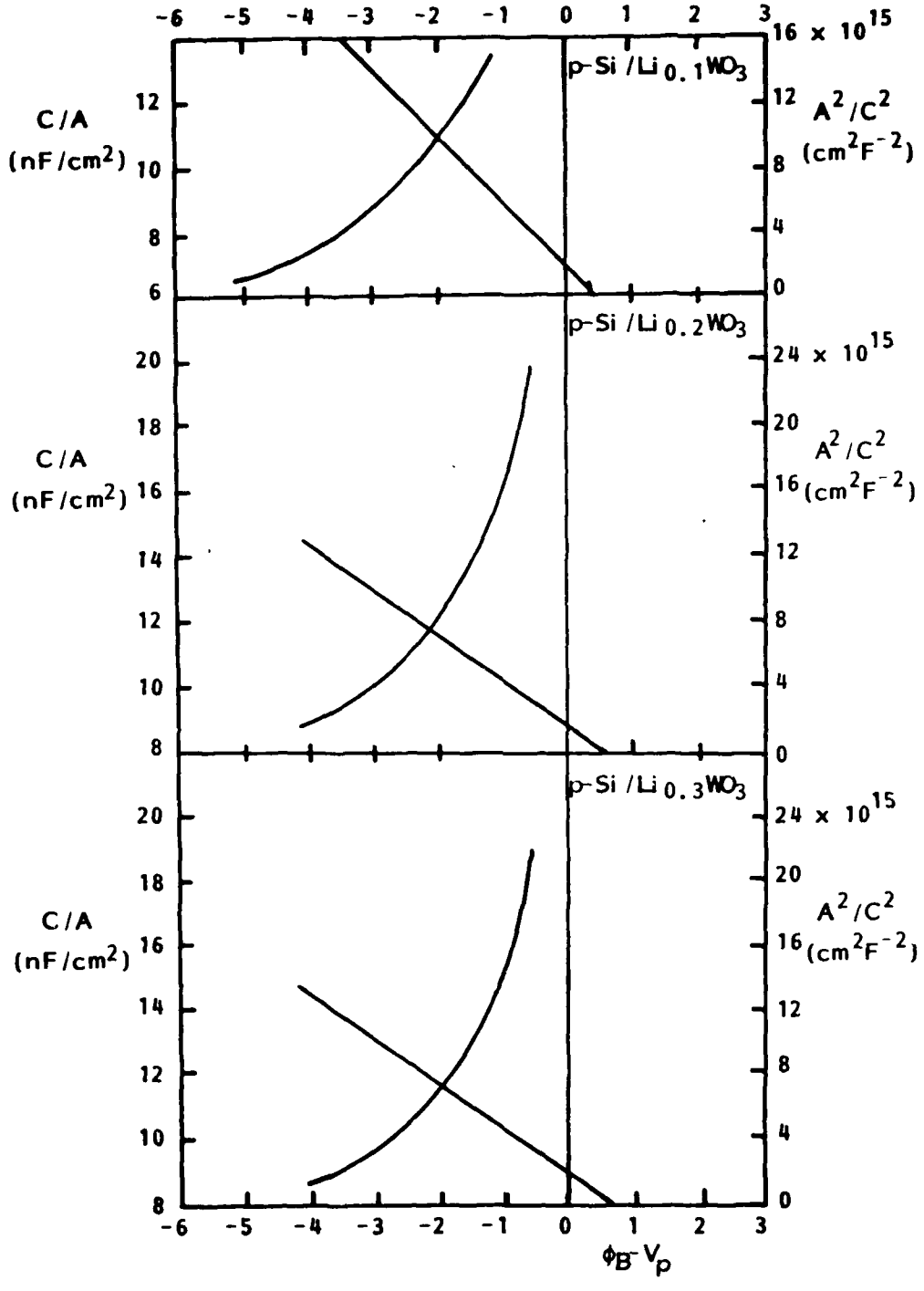

Fig. 5. C-V and $1/C^2$ vs. V plots of p-Si|Li_xWO_3|Ni diodes.

TABLE 2

RESULTS OF CAPACITANCE-VOLTAGE ANALYSIS
OF p-Si/WO_3 DIODES

Diode	Slope($A^2/C^2/V$) ($cm^2\ F^{-1}$)	N_A (cm^{-3})	ϕ_B(eV) (±0.02V) = V_i + V_p
Al|p-Si|Ni	6.2×10^{14}	1.9×10^{16}	0.54 + 0.15 = 0.69
Al|p-Si|WO_3|Ni	4.6×10^{14}	2.6×10^{16}	0.55 + 0.14 = 0.69
Al|p-Si|Li_xWO_3|Ni			
x = 0.1	4.0×10^{15}	2.9×10^{15}	0.50 + 0.20 = 0.70
x = 0.2	2.3×10^{15}	5.1×10^{15}	0.53 + 0.18 = 0.71
x = 0.3	2.1×10^{15}	5.6×10^{15}	0.55 + 0.18 = 0.73
x = 0.4	2.9×10^{15}	4.1×10^{15}	0.56 + 0.20 = 0.76

3.3 Current-Voltage Behavior

Again, all diodes show rectifying behavior. The forward current for a Schottky barrier is given by

$$J = J_s\left(e^{qV/kT}-1\right) \qquad [7]$$

Thus, lnJ vs. applied V will yield a straight line with intercept $\ln J_s$, the saturation current density. At any temperature, T, J_s is related to the barrier height by

$$J_s = A^{**}T^2 \exp\left(-\frac{q\phi B_p}{kT}\right) \qquad [8]$$

where A^{**} is the effective Richardson constant for holes. Plots of $\ln J_f$ (foward current) vs. voltage are shown in Figure 6. The magnitudes of forward currents at a given voltage are inversely related to Li content, as would be expected for increasing barrier height. The plots of $\ln J_f$ vs. V are only classically linear up to ~+0.2V, where diode quality factors of 1-1.5 are calculated. Extrapolation back to 0V yields barrier heights of 0.54 to 0.62V for x(Li) = 0 to 0.4.

The barrier height of a metal-semiconductor contact in which surface states are present at the interface is approximately given by the expression (11):

$$\phi B_p \simeq C_2(\phi_m-\chi) + (1-C_2)\left(\frac{E_g}{q} - \frac{\Delta E_{ss}}{q}\right) \qquad [9]$$

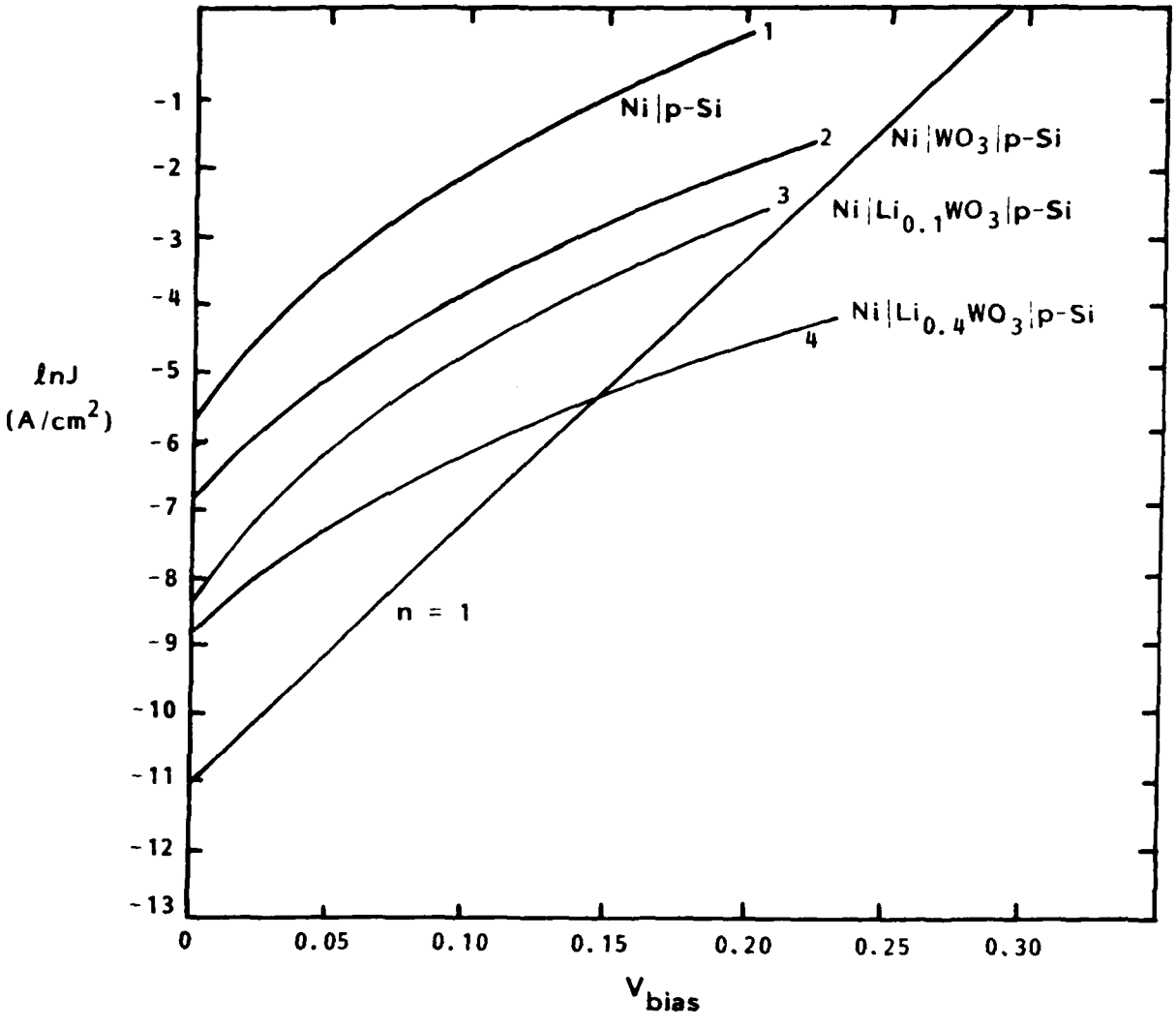

Diode	ℓn J_s	J_s (A/cm^2)	ϕ_B (eV)
1	-4.7	9.1×10^{-3}	0.54
2	-6.0	2.5×10^{-3}	0.58
3	-7.1	8.3×10^{-4}	0.62
4	-8.1	3.0×10^{-4}	0.64

Fig. 6. Representative forward current characteristics for p-Si|Li_xWO_3|Ni Schottky barrier diodes. n = 1 shows ideal diode behavior.

In equation [9], ϕB_p is the barrier height for a p-type semiconductor, ϕ_m is the metal work function, χ is the semiconductor electron affinity, E_g is the band gap of the semiconductor, and ΔE_{ss} is the midpoint energy of the surface state distribution relative to the valence band edge. Many covalent semiconductors have ΔE_{ss} at ∿1/3 of the band gap energy measured from the valence band edge. The coefficient C_2 relates to the interface state density, D_s, and is given as

$$C_2 \equiv \frac{\varepsilon_i}{\varepsilon_i + q^2 \delta D_s} \qquad [10]$$

Here, ε_i is the permittivity of the interfacial layer (usually approximated as ε_o, the free space value) and δ is that layer's thickness, i.e., ∿5Å for an atomic monolayer. We note that if $C_2 = 0$, then the Fermi level is completely pinned at $(E_g - \Delta E_{ss})/q$; if $C_2 = 1$, then the Schottky barrier exhibits classical behavior.

The reversible potentials of the Li_xWO_3 layers, measured electrochemically, span the range -0.4 to +0.4 vs. NHE, or 4.2 to 5.2V vs. vacuum. In Figure 7, a plot of barrier height from equation [8] vs. work function of Li_xWO_3 yields an intercept of 0.85 (typical of p-Si) and a slope of 0.06. The error bars signify the range of barrier height obtained for 5-10 diodes (see Figure 2). The slope, (C_2), is related to the surface state density by $N_{ss} \simeq 1.1 \times 10^{13} (1-C_2)/C_2$. A surface state density of $N_{ss} = 1.7 \times 10^{14}$ cm^{-2} eV^{-1} is thus indicated. The small variation of barrier height with work function and this high surface state density indicates a large degree of Fermi level pinning in the p-Si|Li_xWO_3 interface. A similar slope is obtained from the C-V data.

3.4 Al|p-Si|WO_3 Photoelectrochemical Response

The current-voltage behavior of naked p-Si electrodes in 0.1M HCl was generally nonrectifying, showing high reverse currents and no detectable photocurrent. The p-Si electrodes coated with 3000-4000Å of evaporated WO_3 also showed high forward currents, but also significant superimposed photocurrents when illuminated at 633 nm. Repeated anodic and cathodic sweeps led to rapid passivation of the naked p-Si electrode. The WO_3-coated electrode displayed high currents in both directions, which did not decay (see Figure 8). These are ascribed to the reversible reaction

$$WO_3 + xH^+ + xe^- \rightleftarrows H_xWO_3 \qquad [11]$$

The transient photovoltage was measured as a function of applied voltage using a pulsed dye laser excitation source, and a slowly responding potentiostat for steady state potential control, and a boxcar integrator for capturing and quantifying photovoltages within 10 μsec after the laser firing. In photoelectrochemistry, the photovoltage response

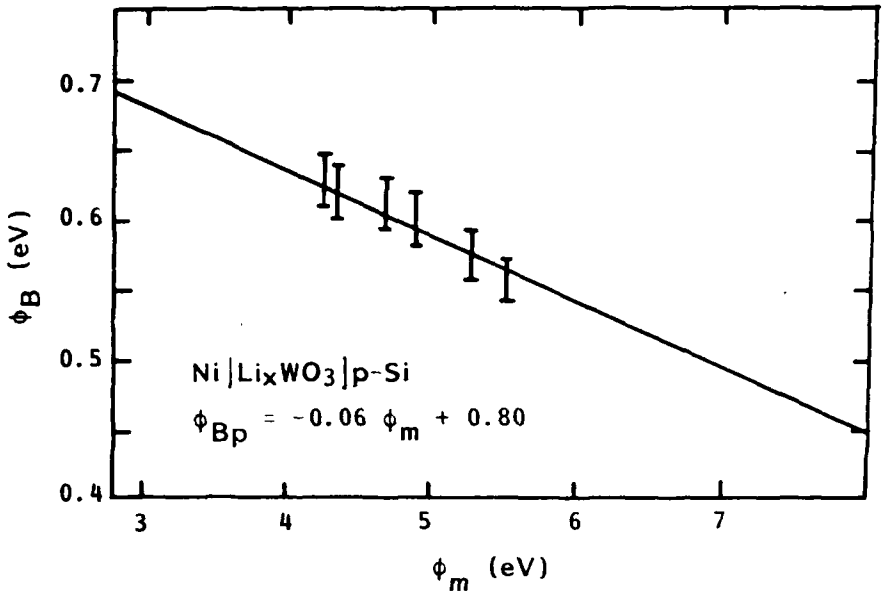

x	V(Li^+/Li)	V(NHE)	ϕ_m [1]	ϕB [2]
Ni	-	-	5.2	0.54
0	3.0	0.4	5.0	0.57
0.1	2.7	0.1	4.7	0.60
0.2	2.5	-0.1	4.5	0.62
0.3	2.35	-0.25	4.35	0.62
0.4	2.2	-0.4	4.2	0.64

[1] ϕ(NHE) $\approx$ 4.6 eV
[2] Obtained from forward current voltage characteristics.

Fig. 7. Variation of barrier height with metal work function (ϕ_m) in Ni|Li_xWO_3|p-Si diodes.

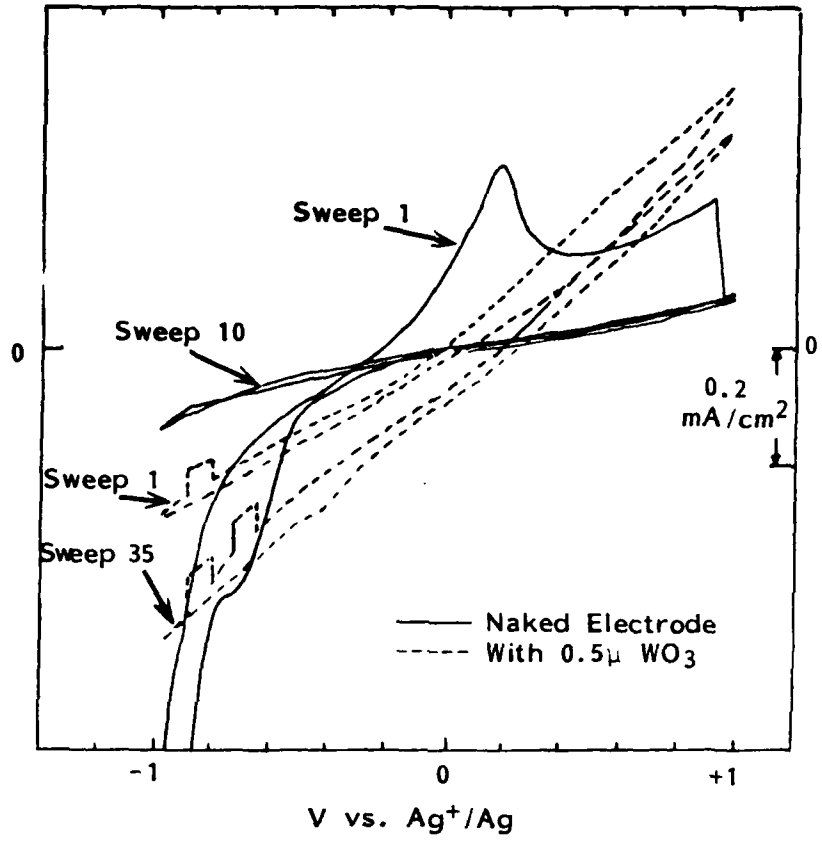

Fig. 8. Current-voltage curves for p-Si (solid line) and p-Si|0.5μ WO_3 (broken line) photocathodes under ∿1 mW/cm² 633 nm illumination. The coated electrode shows a marked photoeffect and high stability. Sweep rate = 10 mV/sec.

is a measure of the band bending, i.e., the fraction of the reverse bias potential dropped across the space charge layer. Under light saturation, ΔV_p vs. V should have a slope approaching unity for an ideal diode.

Figure 9 shows ΔV_p vs. V curves for saturating dye laser pulses at 500 nm ($\sim$100 W/cm^2 pulse). It can be seen that the naked electrode shows a much smaller slope than p-Si/WO_3. Furthermore, the latter electrodes display near unit slopes and a photosensitivity $\sim 10^3$ greater than naked Si. As shown in Figure 10, holding these electrodes at positive bias and thus allowing complete H removal from H_xWO_3 creates a more positive "turn on" potential for the photovoltage, indicating a movement of the band edges with hydrogenation. This is an expected result of a large interface state density between the p-Si surface and the WO_3 layer.

The plots of photovoltage vs. voltage may be transformed to band bending (V_B) vs. voltage when the photovoltage signal is recorded at its maximum value under saturation conditions. At any point on the curves in Figure 10, $(dV_B/dV)_{ST}$ is yielded directly, where ST refers to a static bias. The relationship between this slope and the interface state density, D_s, is given by Fonash (12) as

$$\left(\frac{dV_B}{dV}\right)_{ST} = \left(\frac{1}{1 + C_{sc}/C_I + \alpha'}\right) \qquad [12]$$

Here, C_{sc} is the space charge capacitance, C_I is the capacitance of the interfacial layer containing the surface states, and $\alpha' = q\delta D_s/\varepsilon_i$ (see equation 2). Since $C_I = \varepsilon_i/\delta$, and δ is very thin, then $C_{sc}/C_I \ll 1$, and can be neglected here. We see from Figure 10 that at low bias the slope (dV_B/dV) is small, while at large negative (reverse) bias it approaches a nearly classical value. The flat band potential, V_{FB}, is near zero in all cases except when the electrode was oxidized by holding at 1V for 5 minutes. The initial slopes between V_{FB} and V_{FB}-0.5V are given in Table 3 for p-Si, p-Si|WO_3 and p-Si|$H_{0.1}WO_3$. Values of D_s, calculated from equation [12], are also given.

Although the surface state densities are 5-10 times lower from this analysis than obtained from solid state diodes, Figure 7, the systems are not equivalent in that the photoelectrodes were not annealed in vacuo with Li. The surface states are, nevertheless, high enough to indicate significant Fermi level pinning at low to intermediate band bending. The addition of WO_3 to the naked p-Si surface does tend to decrease D_s, the major effect probably being suppression of p-Si reactivity with the electrolyte. However, we also note that incorporation of H during the scan can have the effect of decreasing the WO_3 work function, thus enhancing the space charge barrier. This effect would add to the observed photovoltage.

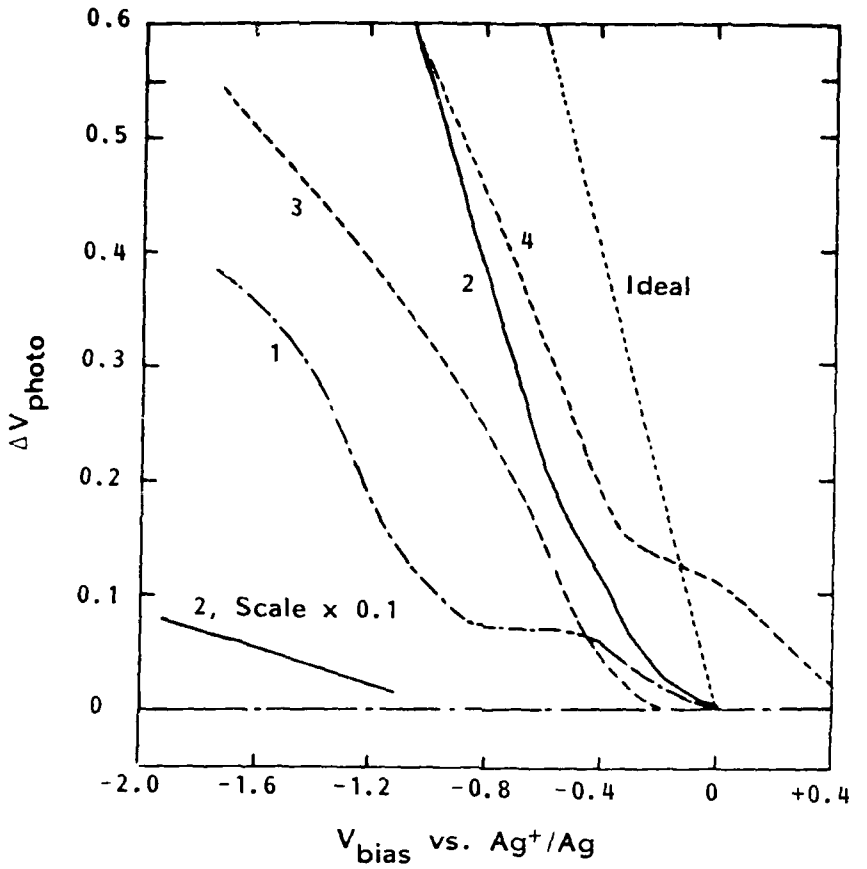

Fig. 9. Photovoltage vs. voltage for p-Si photoelectrodes with and without 0.5 μm WO_3. 1 - Naked electrode; 2 - p-Si| WO_3; 3 - curve 2 repeated at 0.01 x intensity; 4 - curve 3 repeated after holding at +1V for 5 min to remove all H from WO_3. Curves 1 and 2 were recorded at 100 W/cm^2 pulse. All curves recorded at 500 nm.

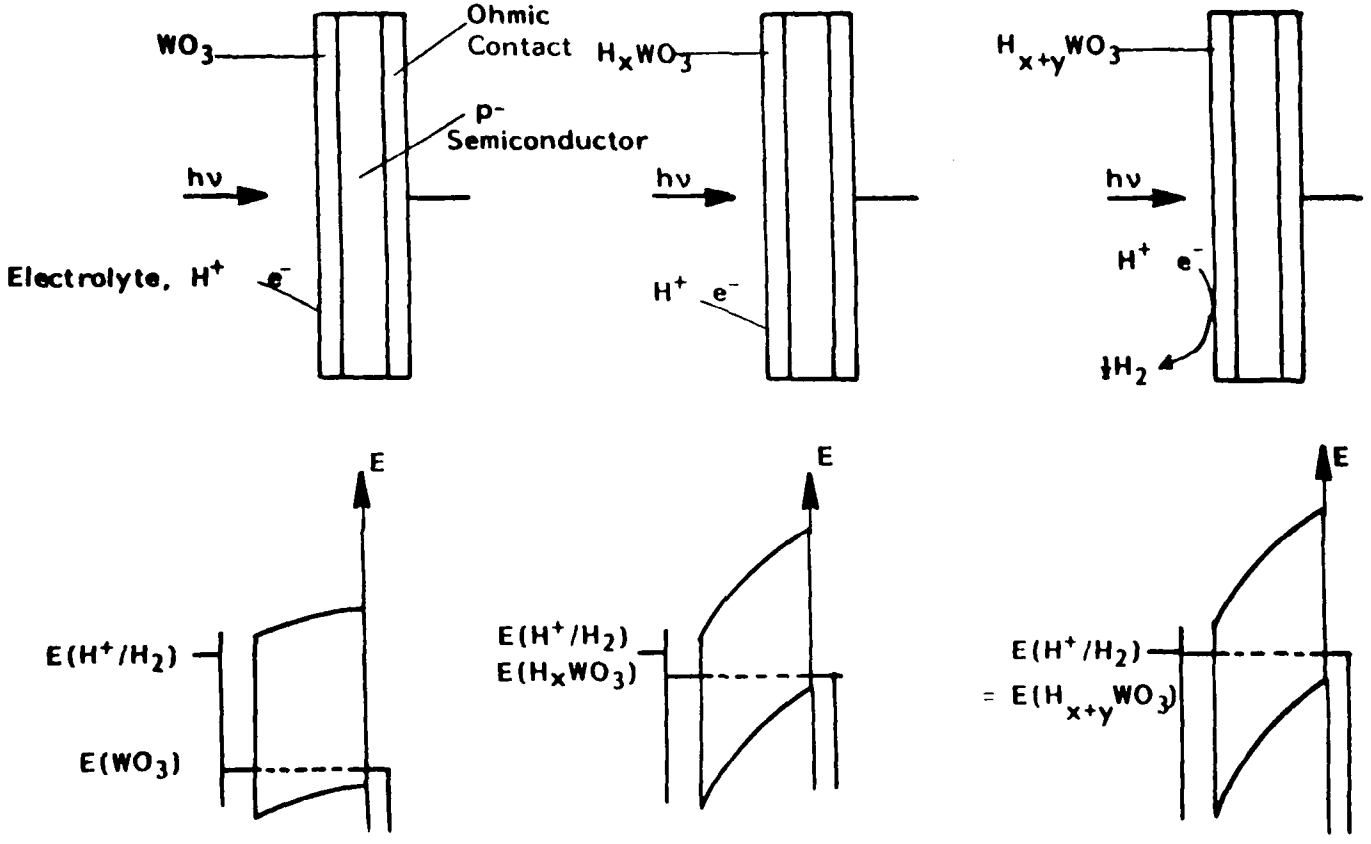

Fig. 10. Development of Schottky barrier during photoelectrochemical reduction of WO_3 overlayer on a p-type semiconductor.

TABLE 3

INITIAL SLOPES OF PHOTOVOLTAGE vs. VOLTAGE CURVES FOR p-Si BASED DIODES IN AQUEOUS 0.1N HCl. ILLUMINATION BY DYE LASER, 100 W/cm^2/ PULSE, PULSE DURATION = 10 nsec, λ = 500 nm. PHOTOVOLTAGE IS RECORDED FROM 1 to 10 μsec AFTER PULSE.

Diode	Initial (dV_B/dV)	D (states/cm^2/eV)
Al|p-Si	0.15	3.1×10^{13}
Al|p-Si|WO_3(0.4 μm)	0.41	7.9×10^{12}
Al|p-Si|$H_{0.1}WO_3$(0.4 μm)	0.65	3.0×10^{12}

This barrier enhancement effect, if confirmed in future research, could be useful in photoelectrochemical H_2 fuel forming reactions on p-type semiconductors. As shown in Figure 10, the H_2 evolution would occur on the WO_3 after it had first become saturated with H_2. A similar enhancement effect has also been considered by Heller and co-workers (13) for Pt|p-InP Schottky barrier photoelectrochemical diodes on formation of the intermetallic compound H_xPt.

4.0 SUMMARY AND CONCLUSIONS

In the Phase I research program, we have identified a new kind of semiconductor barrier element based on the junction formed between a semiconductor and a mixed ionic/electrical conductor with a reversibly variable work function. Such an element can be used to probe the energetics of Schottky barrier formation using a single barrier forming system, rather than employing a variety of Schottky barrier metals, each with its own complex intermetallic chemistry with the underlying semiconductor material.

Also in the Phase I research we were able to conduct preliminary experiments on one model system, the p-Si/M_xWO_3 Schottky barrier. Here, we demonstrated the feasibility of constructing such an element with M = Li and x variable. The results of electrical measurements indicated that interface state density was high over the potential range examined, and Fermi level pinning was dominant. This result is in agreement with the bulk of solid state device literature for p-Si. Larger variations with work function might be expected for barriers with other more ionic semiconductors which are less prone than Si to pinning of the Fermi level near mid-bandgap by surface states. As shown in Figure 11, semiconductors such as CdS and ZnO typically exhibit Schottky barrier heights that are sensitive to metal electronegativity.

In Phase I we suggested the use of such elements in photoelectrochemistry as Schottky barrier photoelectrodes. Here, as shown in Figure 10, the variable work function layer would be employed to maximize the band bending in the semiconductor, while at the same time shielding it from corrosion by the electrolyte. Phase I only permitted us a brief look at H_xWO_3/p-Si as a H_2 evolving photoelectrode, although these results appeared promising. Pt group metal oxides are all variable work function ion insertion compounds, and these in connection with Si, or particularly with more ionic semiconductors, should produce highly efficient catalytic photoelectrodes for H_2 and O_2 evolution.

We recognize that many of the systems considered as insertion compound layers are themselves electrochromic. Thus, photoelectrochemical reactions which employ n-type semiconductors coated with colorless $HIrO_2$, for example, are imagers, viz:

$$\text{n-CdS}\,|\,HIrO_2 \underset{V<V_{fb}}{\overset{h\nu}{\rightleftharpoons}} \text{n-CdS}\,|\,\underset{\text{blue}}{IrO_2} + H^+ + e^- \qquad [13]$$

The degree of reaction would be a function by light intensity, and thus a grey scale could be developed for an imager of submicron resolution.

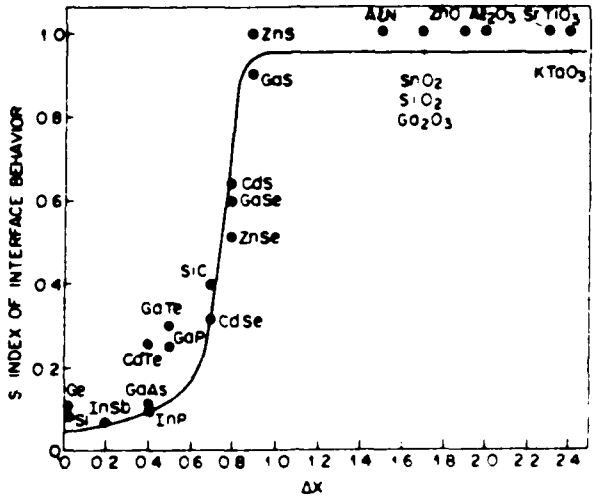

Fig. 11. Index of interface behavior vs. metal-semiconductor electronegativity difference ($\Delta\chi$) for various semiconductors. $S = d\phi_B/d\chi$, where ϕ_B is the barrier height (from Ref. 1).

Finally, we feel that an important application of the proposed work is in the area of chemical and electrochemical sensors. The Phase I research characterizing Schottky barriers has general relevance to this problem since, in order to achieve maximum sensitivity, changes in chemical potential of the chemically sensitive layer must be reflected efficiently as a modulation in semiconductor space charge. In addition, many of the insertion compounds exhibit selectivity with respect to the inserting species. For example, WO_3 undergoes electrochemical reactions of the class

$$xe^- + xM^+ + WO_3 \rightleftarrows M_xWO_3 \qquad [14]$$

where M = H, Li, Na, Ag and where the rates of these reactions vary inversely with the ionic radius of M. Similarly, TaS_2 is a layered compound which reversibly intercalates alkali metals and organic molecules, also with size discrimination and accompanying work function changes.

In conclusion, variable barrier height diodes have numerous applications. Yet, research is at a basic stage. It is crucial to pursue both the science and technology of these elements in order to realize fully their potential benefits in areas of electrochemistry, sensors, imaging, and solid state electronics.

5.0 REFERENCES

1. S. M. Sze, Physics of Semiconductor Devices, 2d ed. (New York: John Wiley & Sons, 1981), Chapter 5.

2. W. C. Dautremont-Smith, Displays, 3, 3 (1982).

3. For a review, see K. M. Abraham, J. Power Sources, 7, 1 (1983).

4. F. R. Gamble, F. J. DiSalvo, R. A. Klemm and T. H. Geballe, Science, 168, 568 (1970).

5. R. H. Micheels and R. D. Rauh, J. Electrochem. Soc., 131, 217 (1984).

6. C. A. Blakney, D. H. Longendorfer, R. A. LeLievre and R. D. Rauh, in Laser Controlled Processing of Surfaces, Materials Research Society, in press.

7. M. Green, Thin Solid Films, 50, 145 (1978).

8. K. H. Cheng and M. S. Whittingham, Solid State Ionics, 1, 151 (1980).

9. M. E. Langmuir, P. Hoening and R. D. Rauh, J. Electrochem. Soc., 128, 2357 (1981).

10. N. Matsuura, K. Umimoto and Z. Takeuchi, Bull. Chem. Soc. Japan, 47, 813 (1974).

11. A. Heller, B. Miller, H. J. Lewerenz and K. J. Bachman, J. Am. Chem. Soc., 102, 6555 (1980).

12. S. J. Fonash, J. Appl. Phys., 54, 1966 (1983).

13. A. Heller, E. Aharon-Shalom, W. A. Bonner and B. Miller, J. Am. Chem. Soc., 104, 6942 (1982).

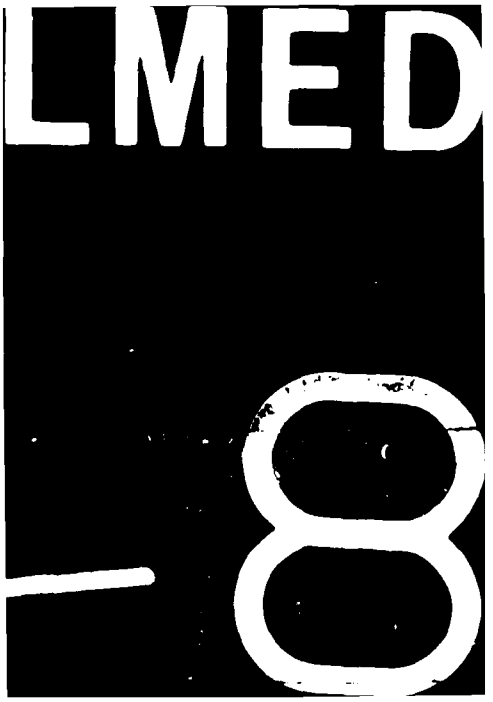
LMED
8